Journal of Advanced Research 39 (2022) 275–289

Contents lists available at ScienceDirect

Journal of Advanced Research

journal homepage: www.elsevier.com/locate/jare

Transcription factor Meis1 act as a new regulator of ischemic arrhythmias in mice

Yining Liu [a,1], Jiamin Li [a,1], Ning Xu [a], Hang Yu [a], Liling Gong [a], Qingsui Li [a], Zhenyu Yang [a], Sijia Li [a], Jiming Yang [a], Di Huang [a], Yadong Xue [a], Genlong Xue [a], Jiali Liu [a], Haixin Chen [a], Ruijie Zhang [a], Anqi Li [a], Yiming Zhao [a], PengYu Li [a], Ming Li [a], Mingbin Liu [a], Ning Wang [a,*], Benzhi Cai [a,b,*]

[a] Department of Pharmacology (State-Province Key Laboratories of Biomedicine-Pharmaceutics of China, Key Laboratory of Cardiovascular Medicine Research, Ministry of Education), College of Pharmacy, Harbin Medical University, Harbin 150081, China
[b] Department of Pharmacy, The Second Affiliated Hospital of Harbin Medical University (Institute of Clinical Pharmacy, The University Key Laboratory of Drug Research, Heilongjiang Higher Education Institutions), Harbin, China

HIGHLIGHTS

- The reduction of Meis1 after MI leads to an increased susceptibility to arrhythmia.
- Meis1 deficiency is related to ubiquitination proteasome pathway mediated by CDC20.
- Meis1 acts as a new transcription activator for *SCN5A* in cardiomyocytes.
- After Meis1 recovery, the electrophysiological function in cardiomyocytes are improved.
- Meis1 is a new target for the treatment of arrhythmia after myocardial infarction.

GRAPHICAL ABSTRACT

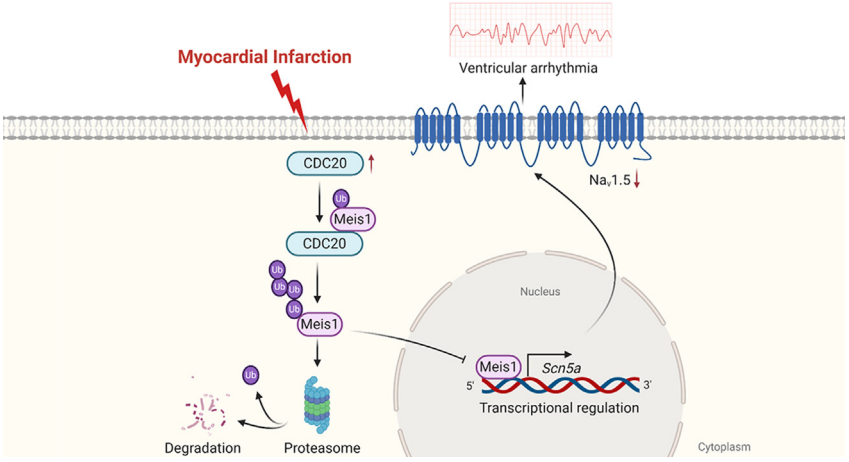

ARTICLE INFO

Article history:
Received 29 August 2021
Revised 25 October 2021
Accepted 10 November 2021
Available online 15 November 2021

Keywords:
Meis1
Ventricular arrhythmias
Myocardial infarction
Na$_V$1.5 channel
CDC20
Ubiquitin

ABSTRACT

Introduction: The principal voltage-gated Na^+ channel, Na$_V$1.5 governs heart excitability and conduction. Na$_V$1.5 dysregulation is responsible for ventricular arrhythmias and subsequent sudden cardiac death (SCD) in post-infarct hearts. The transcription factor Meis1 performs a significant role in determining differentiation fate and regenerative capability of cardiomyocytes. However, the functions of Meis1 in ischemic arrhythmias following myocardial infarction (MI) are still largely undefined.
Objectives: Here we aimed to study whether Meis1 could act as a key regulator to mediate cardiac Na^+ channel and its underlying mechanisms.
Methods: Heart-specific Meis1 overexpression was established by AAV9 virus injection in C57BL/6 mice. The QRS duration, the incidence of ventricular arrhythmias and cardiac conduction velocity were evaluated by ECG, programmed electrical stimulation and optical mapping techniques respectively. The conventional patch clamp technique was performed to explore the I_{Na} characteristics of isolated mouse ventricular myocytes. *In vitro,* Meis1 was also overexpressed in hypoxic-treated neonatal

Peer review under responsibility of Cairo University.

* Corresponding authors at: Department of Pharmacology (State-Province Key Laboratories of Biomedicine-Pharmaceutics of China, Key Laboratory of Cardiovascular Medicine Research, Ministry of Education), College of Pharmacy, Harbin Medical University, Harbin 150081, China (N. Wang).
E-mail addresses: wangning@ems.hrbmu.edu.cn (N. Wang), caibz@ems.hrbmu.edu.cn (B. Cai).

[1] The first two authors contributed equally to this work.

https://doi.org/10.1016/j.jare.2021.11.004
2090-1232/

Nomenclature

Nonstandard Abbreviations and Acronyms

AMI	Acute Myocardial infarction
AAV9	Serotype 9 adeno-associated virus
AP	Action potential
CDC20	Cell division cycle 20 homologue
ES	Electrical Stimulation
LV	Left Ventricle
LAD	left anterior descending
MI	Myocardial infarction
NC	Negative Control
SCD	Sudden cardiac death
UPS	Ubiquitin proteasome
VF	Ventricular Fibrillation
WT	Wild-type

cardiomyocytes. The analysis of immunoblotting and immunofluorescence were used to detect the changes in the expression of $Na_V1.5$ in each group.

Results: We found that forced expression of Meis1 rescued the prolongation of QRS complex, produced anti-arrhythmic activity and improved epicardial conduction velocity in infarcted mouse hearts. In terms of mechanisms, cardiac electrophysiological changes of MI mice can be ameliorated by the recovery of Meis1, which is characterized by the restoration of I_{Na} current density and $Na_V1.5$ expression level of cardiomyocytes in the marginal zone of MI mouse hearts. Furthermore, in vitro studies showed that Meis1 was also able to rescue hypoxia-induced decreased expression and dysfunction of $Na_V1.5$ in ventricular myocytes. We further revealed that E3 ubiquitin ligase CDC20 led to the ubiquitination and degradation of Meis1, which blocked the transcriptional regulation of *SCN5A* by Meis1 and ultimately led to the electrophysiological remodeling in ischemic-hypoxic cardiomyocytes.

Conclusion: CDC20 mediates ubiquitination of Meis1 to govern the transcription of *SCN5A* and cardiac electrical conduction in mouse cardiomyocytes. This finding uncovers a new mechanism of $Na_V1.5$ dysregulation in infarcted heart, and provides new therapeutic strategies for malignant arrhythmias and sudden cardiac death following MI.

Introduction

Ventricular arrhythmias represent one of the leading causes of morbidity and mortality in patients with acute myocardial infarction (AMI) [1]. The survivors of AMI still have an increased risk of ventricular arrhythmias and sudden cardiac death, mainly due to ion channels remodeling and cardiac electrical abnormalities in MI [2]. Although traditional antiarrhythmic drugs are capable to alleviate arrhythmias to a certain extent, their negative inotropic and arrhythmogenic effects cannot be ignored [3]. Voltage-gated cardiac Na^+ current (I_{Na}) carried by the *SCN5A*-encoded $Na_V1.5$ α subunit acts a pivotal part in the electrical conduction and excitability of the heart by regulating the depolarization process of cardiac action potential (AP) [4–5]. The dysfunction of intracellular Na^+ channels has been shown to be a critical predisposing factor for life-threatening ventricular arrhythmias [6–8]. It was reported that the functional impairment or down-regulation of $Na_V1.5$ could slow down the conduction velocity of the infarcted heart, which was related to the death in heart failure and cardiomyopathies [9–10]. In addition, genetic analysis revealed that mutations of *SCN5A* are associated with multiple arrhythmogenic diseases such as Brugada syndrome and Long QT syndrome [11]. However, at present, our understanding of molecular mechanisms of cardiac Na^+ channel dysfunction after MI is still inadequate. To define the potential mechanism of cardiac Na^+ channel dysfunction after MI is of great significance for the therapy of post-infarcted arrhythmias.

The transcription factor Meis1 is a member of the homeobox gene family, and has emerged as a key regulator of a wide range of biological activities including cell cycle, oxidative stress, differentiation and embryonic development [12–15]. In hearts, Meis1 level was altered in postnatal and post-infarcted hearts, which has been shown to cause the loss of cardiac regenerative ability in mice [14,16]. Notably, A recent study found that the loss of transcription factor Meis1 increases the sensitivity to sudden cardiac death by inhibiting the sympathetic neurons target-field innervation [17]. In addition, two large-scale genomic association studies showed that gene mutation in Meis1 is correlated with abnormal PR interval in patients [18–19]. It has been well documented that prolongation of the PR interval is a significant indication of atrial and atrioventricular nodal conduction block in patients [20]. It suggests that Meis1 might be involved in the regulation of cardiac conduction and heart rhythm. However, whether Meis1 performs a regulatory part in cardiac Na^+ channel and thus participates in the occurrence of arrhythmias after MI has not elucidated yet.

Accumulating evidence indicated that the post-translational modification of ubiquitin proteasome system (UPS) is largely responsible for protein degradation [21]. Recent studies have shown that the dysfunction of UPS is recognition as a potentially important mechanism involved in the onset and development of various cardiac diseases [22–23]. In the process of ubiquitin proteasome, E3 ligase as a key enzyme, specifically recognizes ubiquitinated protein substrates. Cell division cycle 20 homologue (CDC20) performs an essential role in the progression of the cell cycle via activating the anaphase promoting complex (APC) E3 ubiquitin ligase which causes the ubiquitination and degradation of specific substrates [24–25]. Recently, it was reported that CDC20 mediates PPM1K regulation of Meis1 in hematopoiesis and leukemogenesis [26]. Additionally, database analysis studies have found that CDC20 was significantly enriched in rat cardiomyocytes after myocardial infarction, which indicates that CDC20 might participate in the development of myocardial ischemia [27]. However, whether CDC20 also plays a vital role on Meis1 during the course of ischemic arrhythmia and its molecular mechanism need to be further identified.

Although previous studies afforded growing evidences to support the role of sodium channel in the progress of ischemic arrhythmias caused by MI, the role of ubiquitin proteasome system and transcription factors in cardiac electrical remodeling after MI

are still missing. Therefore, we conducted the present study to investigate the regulatory roles of Meis1 in cardiac electrical conduction and arrhythmias in the mouse MI model and elucidate its underlying mechanisms. Our results firstly showed that Meis1 acts as a transcription activator for *SCN5A* and prevent the $Na_V1.5$ down regulation from MI injury. The reduction of Meis1 after MI leads to an increased susceptibility to arrhythmia, and this deficiency is associated with ubiquitination proteasome degradation.

Materials and methods

Ethics statement

All animal experiments were conducted in accordance with the NIH guidelines (Guide for the care and use of laboratory animals, NIH Publication No. 85-23, revised 1996) and the whole experimental process were carried out according to the procedures approved by the Institutional Animal Care and Use Committee of Harbin Medical University.

AAV9-GFP construction and tail vein injection

Recombinant adeno-associated virus serotype 9 (AAV9) vectors carrying the cardiac troponinT (cTNT) promoter driving the expression of enhanced green fluorescent protein (AAV9-cTNT-GFP) and Meis1 (AAV9-cTNT-GFP-Meis1) were provided by Hanbio Biotechnology Co.,Ltd (Shanghai, China). The backbone vector AAV9-cTNT-GFP was used as a control (AAV9-NC). AAV9-cTNT-GFP-Meis1 (AAV9-Meis1), which can drive strong, cardiomyocyte-selective expression of Meis1 were injected into the tail vein at a dose of 1.3×10^{11} viral genomes (vg) per animal. Four weeks after carrier administration, the mice hearts were subjected to cryosection and then fluorescence microscopy was used for GFP distribution detection. In addition, AAV9-shMeis1/NC were administered to mice using the same method and dose as above to construct Meis1 knockdown in cardiomyocytes.

Animal models

Male C57BL/6 mice (20–25 g) were maintained on a 12 h light/-dark cycle at 22 °C and 55–60% humidity. The animals were randomized into the following three groups: sham, MI + AAV9-NC and MI + AAV9-Meis1 group. The left anterior descending branch of the mouse coronary artery was ligated to construct a model of myocardial infarction, which was consistent with the previous procedure [28]. In brief, mice were anesthetized in the gas chamber with 2–4% isoflurane (MIDMARK, USA) and ventilated by orotracheal intubation. A left thoracotomy was performed to expose the heart and the coronary artery of left anterior descending (LAD) was ligated by a 7-0 prolene suture. Ischemia is confirmed by ST-segment elevation in ECGs and sudden local pallor of the myocardium. The mice in the sham group underwent the same procedure except for LAD ligation. AAV9 was injected into the tail vein after the operation at a dose of 1.3×10^{11} viral genomes (vg) per animal. Four weeks after carrier administration, the animals were euthanized by cervical disarticulation while the mice were under a surgical platform of anaesthesia after isoflurane induced unconsciousness and the hearts were extracted for detection of various indicators.

Electrocardiogram

The recording of surface standard lead II electrocardiogram (ECG) in mice of each group was performed on the biometric signal acquisition and analysis system (BL-420S, Chengdu Taimeng, China) with bipolar limb leads. Briefly, after the mice were anesthetized, two electrodes were inserted under the surface of the limbs, and then were connected to the electrocardiograph. The signals were recorded for 15 min at a frequency response of 0.05–500 Hz, followed by digitally analyzed in the BL-420S system.

Intracardiac electrophysiological recordings

Four weeks after the MI operation, the intracardiac electrophysiological recordings were performed in mice of each group. After being anesthetized with isoflurane, the mice were fixed on a heated operating table to maintain a body temperature of 37 °C. A 1.1 F octapolar electrophysiology catheter (FTS-1113A-0518; Scisense, California, USA) was inserted into the right ventricle via the jugular vein and used to induce ventricular arrhythmias between 100 and 400 Hz. The electrical stimulation of the program was performed using a current pulse provided by an external stimulator (STG3008, multichannel system, Reutlingen, Germany). Right ventricle pacing protocol consisted of 10 basal stimuli and 1 subsequent additional stimulus. The cycle lengths of basal stimulation were 80 ms and the extra stimulation were 60 ms and the interval length was successively shortened every 2 ms until the ventricular arrhythmias were induced. The Surface electrocardiograms and intracardiac electromyograms were recorded and analyzed with the LabChat throughout the experiment. Ventricular fibrillation was characterized by five or more consecutive irregular fluctuations.

Optical mapping

The mice were heparinized firstly to prevent clotting and anesthetized with isoflurane. The hearts were removed and washed immediately with oxygenated Tyrode's solution (in mM: 127 NaCl, 1.54 NaH_2PO_4, 20 $NaHCO_3$, 1.0 $MgCl_2{\cdot}6H_2O$, 4.7 KCl, 1.72 $CaCl_2$ and 11.1 glucose in deionized water, adjusts pH to 7.4) at a constant temperature of 37 °C. After aortic catheterization, the heart was perfused retrogradely with Tyrode's solution. (-)-Blebbistatin (10 μmol/L, Selleckchem, Houston, TX, USA) was used to inhibit the cardiac contractility, after which the potentiometric probe RH237 (Invitrogen, Carlsbad, CA) was mixed into the Tyrode's solution and perfused into the mouse heart for 10 min. The heart was excited by the light source of green LED lamp (530 nm), followed by an electrode was placed at the tip of the left ventricle for stimulation at different frequencies. The fluorescence images were captured with the CMOS camera (MiCAM05 Ultima, SciMedia, California, USA) by 1000 frames per second and 100×100 pixels. SciMedia customized software (SciMedia, Costa Mesa, CA) was used to initiate fluorescence signal recording and statistics of cardiac conduction velocity.

Patch clamp recordings

Sodium currents in mice ventricular myocardium was recorded with whole-cell patch clamp recording technique as described previously [9,29]. All whole-cell patch-clamp recordings were conducted at room temperature (23 ± 1 °C) using a patch clamp amplifier (MultiClamp 700B; Axon Instruments Inc., Foster City, CA, USA). The ionic currents were measured in the voltage-clamp mode and the electrode resistance was 2–4 MΩ. The isolated ventricular myocyte suspension was added to the bath placed in an inverted microscope (IX-70; Olympus) and then Tyrode solution was injected. The Tyrode solution for I_{Na} containing the following (in mM): 1.5 $MgCl_2$, 5 HEPES, 4.5 CsCl, 1 $CaCl_2$, 5 D-glucose, 0.1 $CdCl_2$ and 145 NaCl (adjust the pH to 7.37 with CsOH), and the pipette solution containing (in mM): 20 CsCl, 10 EGTA, 110 CsF, 10 HEPES and 10

NaF (adjust the pH to 7.20 with CsOH). The data were acquired and digitized by using Digidata 1440 converter (Axon Instruments Inc., Foster City, CA, USA) and pCLAMP 10.6 software (Axon Instruments Inc., Foster City, CA, USA) and stored on a computer. Data evaluation was conducted through the usage of pClampfit 10.4 software program (Axon Instruments Inc., Foster City, CA, USA).

Neonatal mouse primary cardiomyocyte culture

Neonatal primary cardiomyocytes were dissociated from 1 to 3-day-old SPF-grade mice hearts. In brief, cardiomyocytes were isolated using a selective adherent technique after digestion with 0.25% trypsin solution. Cardiomyocytes were cultured in DMEM with 10% fetal bovine serum, 1% penicillin and streptomycin in an atmosphere of 5% CO_2 and 95% air at 37 °C for 48 h. The Meis1 plasmid, negative control (NC) was synthesized by GenePharma (Shanghai, China), which were transiently transfected using Lipofectamine2000™ transfection reagent (Invitrogen, Carlsbad, CA, USA). After 24 h of transfection, the cells were moved to an anoxic chamber (1% O_2, 5% CO_2) for 24 h to take the hypoxic stimulation.

Western blot analysis

Western blot was conducted to test the protein levels in mouse ventricular tissue and neonatal cardiomyocytes. We take the 2 mm area around the infarct of the pathological mouse heart as the *peri*-infarcted region. After quantification with the BCA Protein Assay kit (Beyotime, Shanghai, China), an equal amount of 60 μg protein from each group was fractionated by 8% SDS-PAGE and electroblotted onto NC membranes (Pall, New York, USA). Membranes were incubated with primary antibodies overnight at 4 °C, including rabbit anti-Meis1 antibody (Abcam, UK, Cat#: ab19867, 1:1000), rabbit anti-$Na_v1.5$ antibody (Alomane laboratory, Israel, Cat#: ASC-005, 1:200), mouse anti-CDC20 antibody (Proteintech Group, America, Cat#: 10252-1-AP, 1:500), mouse anti-Ub antibody (Santa Cruz Biotechnology, Europe, Cat#: sc-8017, 1:1000), mouse anti-His antibody (Santa Cruz Biotechnology, Europe, Cat#: sc-57598, 1:200) and mouse anti-flag antibody (Sigma, USA, Cat#: F1804, 1:1000). Mouse anti-β-Actin antibody (Zhongshanjinqiao, Beijing, China, Cat#: TA-09, 1:1000) was used as an internal reference. The Odyssey CLx Infrared Imaging System (LI-COR Biosciences, Lincoln, Nebraska, USA) was used for image capture and Image studio software was used to quantify bands in each group.

RNA extraction and RT-qPCR analysis

Total RNA extractions from mouse ventricular tissues and cultured primary cardiomyocytes were performed using Trizol™ Reagent (Invitrogen, USA) and measured on NanoDrop-2000 spectrophotometer. Reverse-cDNA synthesis was performed by ReverTra Ace qPCR RT Kit (TOYOBO, Japan) and SYBR Green PCR Master Mix (Dojima Hama, 2-Chome, Kita-kuOsaka, Japan) was used for performing mRNA quantification. The real-time PCR was performed using the 7500 FAST Real-Time PCR System (Applied Biosystems, Waltham, MA USA) and GAPDH was used as an internal control to normalize the expression levels of mRNA. The primers sequences of this experiment are listed in Table 1.

Immunofluorescence staining

Neonatal cardiomyocytes of each group were fixed in 4% paraformaldehyde (PFA) for 30 min at room temperature. After permeabilized with 0.5% Triton X-100 for 15 min and blocked with goat serum for 1 h, the samples were co-incubated with antibodies anti-$Na_v1.5$ (Alomane laboratory, Israel, Cat#: ASC-005, 1:200) and anti-α-actinin (ab50599, Abcam, Cambridge, UK, 1:100) overnight at 4 °C. Then, cardiomyocytes were incubated with secondary antibody for 1 h at 37 °C in darkness, followed by nuclei staining of DAPI (Beyotime, Shanghai, China, 1:1000) for 10 min. A confocal laser scanning microscope (Zeiss, Oberkochen, Germany) was used to captured the immunofluorescence images.

Table 1
The primers sequences for real-time quantitative PCR.

Gene	Forward primer	Reverse primer
Meis1	5′-TCCCAAAGTAGCCACCAATATC-3′	5′-CTGTATCTGTGCCAACTGCTT-3′
$Na_v1.5$	5′-CAACCAGACAGAAGGGGACC-3′	5′-GCTGCTCCTCATACCCTCTG-3′
CDC20	5′-CATTCACTCAACATCAAGGCG-3′	5′-ATGGAGCACACCTGGGAAT-3′
GAPDH	5′-AAGAAGGTGGTGAAGCAGGC-3′	5′-TCCACCACCCAGTTGCTGTA-3′

Immunohistochemistry

Tissue samples were fixed with 10% formalin and embedded in paraffin. Six micrometer sections were cut from paraffin-embedded heart tissues for subsequent experiments. Sections were deparaffinized through Xylene, quenched endogenous peroxidase activity with 3% H_2O_2 for 10 min. Antigen repairment was performed by heating sodium citrate buffer at 99 °C for 10 min. After natural cooling, the sections were blocked with 5% BSA for 27 min in 37 °C, and then incubated with anti-Meis1 antibody (Abcam, UK, Cat#: ab19867, 1:1000) at 4 °C overnight, rinsed for 5–10 min in PBS and incubated for 1 h with the second antibody at 37 °C. The slides were stained by 3, 3′-diaminobenzidine (DAB) solution. Immunohistochemistry images were captured by a microscopy (Olympus BX53, Japan).

Co-immunoprecipitations

A total of 1000 μg protein from the primary cultured cardiomyocytes were cleaved by Radio Immunoprecipitation Assay (RIPA) lysis buffer and incubated with 1.0 μg primary antibody at 4 °C overnight. After that, 35 μL protein A/G PLUS agarose beads (Santa Cruz) were mixed into the compound which continued to shake overnight. The beads were washed with ice-cold TBST buffer for 3 times after centrifugation. Next, 100 μL 1 × loading buffer was added into the precipitation and after that the samples was boiled for 10 min and centrifuged. Finally, the supernatant was taken for Western blot analysis.

Statistical analysis

Data are presented as mean ± SEM. Two-tailed Student's *t*-test was used to compare the differences between the two experimental groups and ANOVA was used to compare the difference among multiple groups. *P* value less than 0.05 was defined as statistical significance. All statistical analyses were carried out using GraphPad Prism 8.0 (GraphPad Software Inc., San Diego, CA).

Results

Meis1 is down-regulated in cardiomyocytes from the border zone of MI hearts

To assess the potential involvement of Meis1 in post-infarcted arrhythmias, the expression of Meis1 was firstly analyzed in MI mouse hearts and hypoxic cardiomyocytes. Compared with the sham group, the expression level of Meis1 was significantly decreased in the border zone of infarcted hearts (Fig. 1A). The reduction of Meis1 expression was also verified by immunohistochemistry of ventricular myocardium in infarcted mice (Fig. 1B). Consistent with the *in vivo* results, the protein level of Meis1 was

down-regulated in neonatal mouse cardiomyocytes treated with hypoxia (Fig. 1C). In order to further verify whether Meis1 protein change is also present in human cardiomyocytes treated with hypoxia. We examined the Meis1 protein levels in human embryonic stem cells derived cardiomyocytes (hESC-CM) in each group. It was found that Meis1 also decreased in hypoxia-treated hESC-CM (Fig. 1D). The reduced expression of Meis1 in ischemic and hypoxic cardiomyocytes suggests that Meis1 might be involved in the pathological process of myocardial infarction.

Forced overexpression of Meis1 inhibits the susceptibility of ventricular arrhythmias after MI

Based on the above findings, we further explored whether the alteration of Meis1 is related to ischemic arrhythmias by the experimental procedure as shown in Fig. 2A. *In vivo* study, we constructed MI mouse model by the left anterior descending (LAD) coronary artery ligation, and then AAV9-cTNT-GFP (AAV9-NC) and AAV9-cTNT-GFP-Meis1 (AAV9-Meis1) were delivered into MI mouse models via tail vein injection. Four weeks after AAV9-Meis1 infection (1.3×10^{11} vg), the expression efficiency of Meis1 was verified by immunoblotting and GFP fluorescence intensity in various tissues. The results demonstrated that AAV9-Meis1 successfully induced the specific expression of Meis1 in mouse cardiomyocytes rather than other tissues, such as liver, kidney and spleen (Fig. 2B, **Supplementary** Fig. 1A). Furthermore, electrocardiogram investigation showed the prolongation of QRS complex in mice after MI (16.4 ± 0.2 ms in MI + AAV9-NC vs.12.2 ± 0.4 ms in Sham, $P < 0.01$), which indicates the increased susceptibility of ventricular fibrillation and SCD in MI mice. Notably, the QRS prolongation induced by ischemic was markedly reversed in MI + AAV9-Meis1 group (from 16.4 ± 0.2 ms to 13.3 ± 0.4 ms, $P < 0.01$, Fig. 2C).

To further determine the role of Meis1 in the susceptibility of ischemic arrhythmias in mice with MI, we conducted the programmed ventricular stimulation induced representative ventricular fibrillation (VF). The susceptibility of arrhythmia was markedly

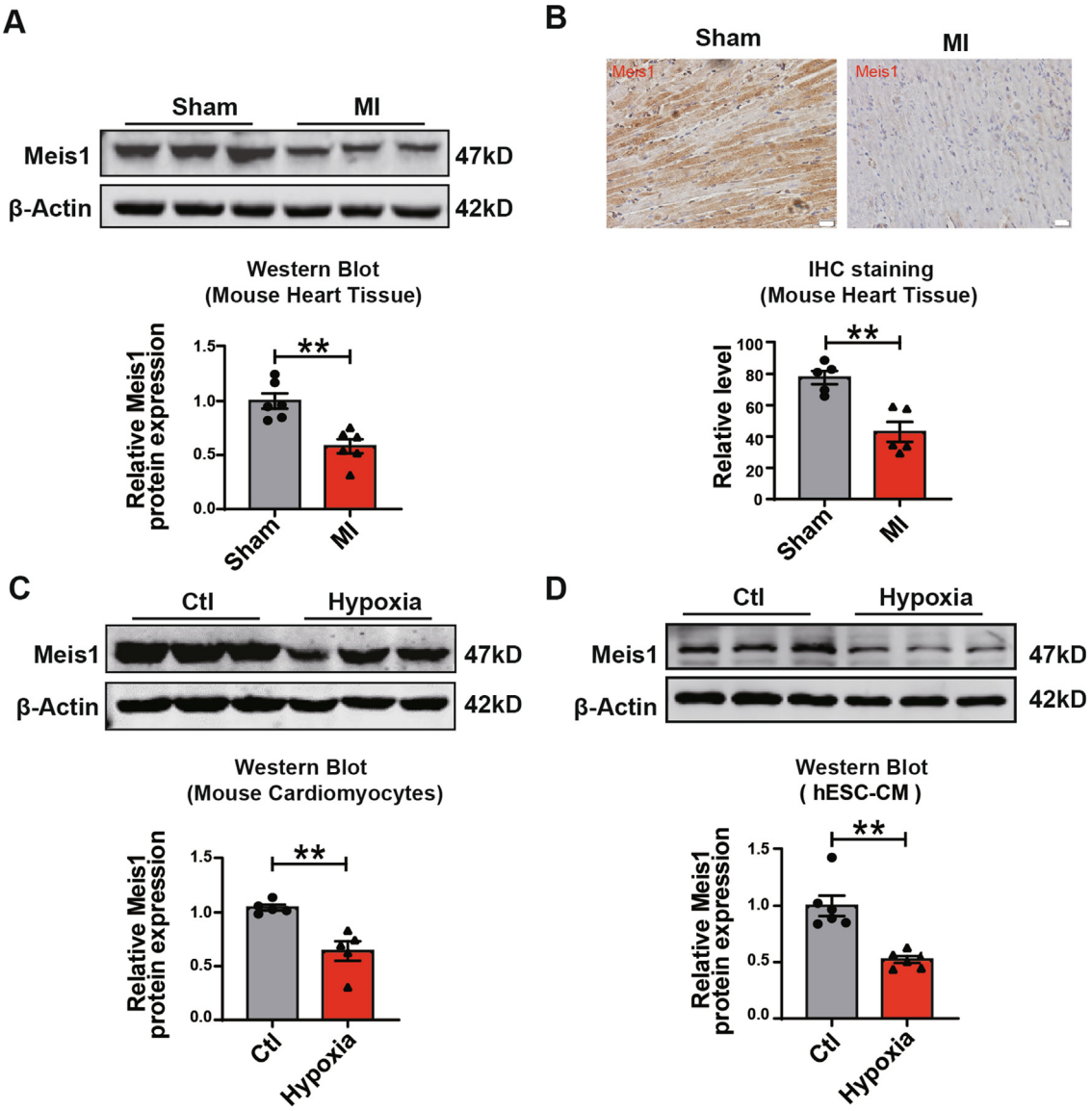

Fig. 1. Meis1 is down-regulated in ischemic cardiomyocytes. **(A)** The protein expression of Meis1 in the border zone of infracted hearts from Sham and MI mice (n = 6). **(B)** Immunohistochemical staining showed that the expression of Meis1 in ventricular myocardium of MI mice was decreased compared with the Sham group (n = 5). Scale bar, 20 μm. **(C-D)** The protein level of Meis1 in neonatal cardiomyocytes and human embryonic stem cells derived cardiomyocytes (hESC-CM) were reduced after treatment with hypoxia for 24 h compared with the Ctl (n = 5–6). Two-tailed Student's *t*-test was used to compare the differences between the two experimental groups. Error bars represent mean ± SEM. $^{**}P < 0.01$.

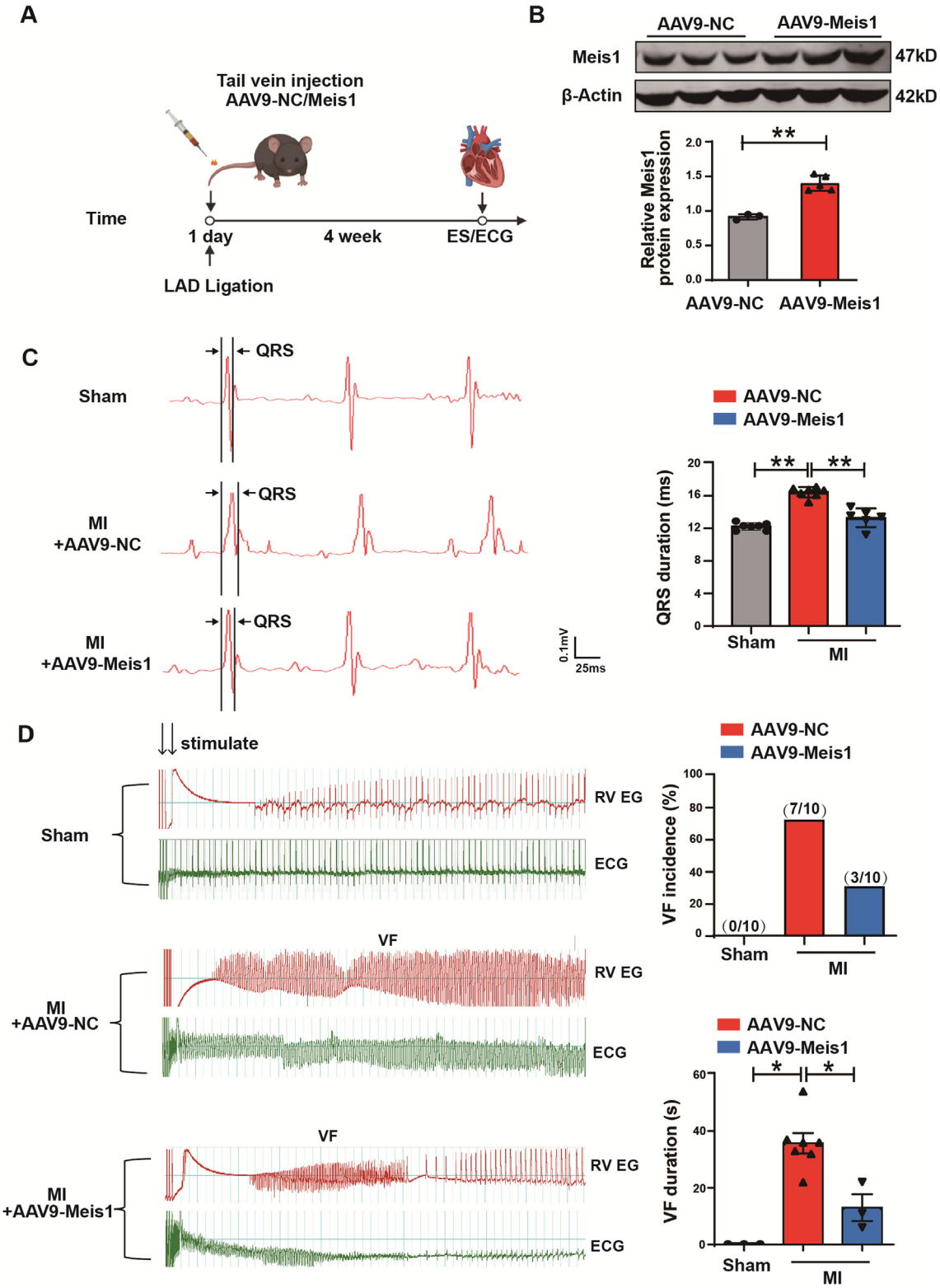

Fig. 2. Meis1 reduces the incidence of ventricular arrhythmias after myocardial infarction. **(A)** Schematic diagram of experimental procedure *in vivo* study. ES: electrical stimulation; ECG: electrocardiogram. **(B)** Compared with AAV9-NC, Meis1 protein level was increased in the hearts of mice in AAV9-Meis1 group, indicating that Meis1 overexpression in cardiomyocytes was successfully constructed (n = 3–5). **(C)** Representative ECG recorded from mice of each group (left panels). QRS complex was shortened in MI + AAV9-Meis1 group (from 16.4 ± 0.2 ms to 13.3 ± 0.4 ms) compared with MI + AAV9-NC mice (right panels, n = 6–8). **(D)** Representative ventricular fibrillation (upper tracing) and ECG (lower tracing) recorded by programmed ventricular stimulation (left panels). The incidence and duration of ventricular fibrillation in each group (right panels, n = 10). This stimulation procedure was repeated 3 times to ensure the reproducibility of the experiment, so as to assess the incidence of ventricular arrhythmia in mice after MI. RV EG: Right ventricular electrocardiogram. VF: ventricular fibrillation. One-way analysis was used to compare the difference among multiple groups. Error bars represent mean ± SEM. $^{*}P < 0.05$, $^{**}P < 0.01$.

elevated as demonstrated by the facilitated induction rate (70%) and extended duration of VF (35.7 ± 3.6 s vs. Sham) in infarcted mouse heart subjected to electrical stimuli. However, VF incidence was lower (from 70% to 30%) in MI + AAV9-Meis1 mice compared with MI + AAV9-NC group. Consistently, the overexpression of Meis1 in MI mice reduced the duration of ventricular fibrillation compared with AAV9-NC-treated MI mice (from 35.7 ± 3.6 s to 13.0 ± 4.7 s, $P < 0.05$, Fig. 2D). These results suggest that Meis1 overexpression inhibits the increased arrhythmic susceptibility in infarcted hearts.

Cardiac specific overexpression of Meis1 improves electrical conduction in mice after myocardial infarction

Abnormal cardiac conduction function is a significant feature of post-MI ventricular arrhythmias. To further characterize the epicardial conduction of the overexpressing Meis1 in the heart, electrophysiological assessment by optical mapping with a voltage-sensitive dye was performed in Langendorff-perfused mouse hearts. A representative activation map obtained by electrode pacing in each group was shown in Fig. 3A. Upon the stimulation with pacing cycle length at 200 ms, electrical conduction velocity (CV) of the ventricle were significantly slowed down in MI mice compared with the sham-operated group (0.29 ± 0.02 m/s vs.0.53 ± 0.03 m/s, $P < 0.01$), and this electrical conduction abnormality was attenuated from 0.29 ± 0.02 m/s to 0.45 ± 0.02 m/s in AAV9-Meis1 infected MI mice (Fig. 3 **B**).

It is properly acknowledged that sodium current (I_{Na}) is an established key factor for cardiac excitability and impulse propagation. Therefore, we speculated that the slowdown of cardiac conduction after myocardial infarction noticed in our study may be attributed to the damage of I_{Na} currents. To investigate the effects of Meis1 on I_{Na} currents, we first used conventional patch clamp techniques to study the I_{Na} characteristics of isolated mouse ventricular myocytes. Representative whole-cell sodium current traces recorded from Sham, MI + AAV9-NC and MI + AAV9-Meis1 ventricular cells are showed in Fig. 3C. The current density was obtained via dividing the peak current by the capacitance of single cardiomyocyte. As illustrated in Fig. 3D, the current densities of I_{Na} were obviously reduced in ischemic cardiomyocyte, in contrast to the density of myocardium in sham group mice. Interestingly, in the AAV9-Meis1 mice hearts, current recordings from −40 mV to −15 mV revealed a restoration in reduced I_{Na} current density. At the test potential of −35 mV, the peak current density was −45.7 ± 0.6 pA/pF for Sham, −25.0 ± 2.3 pA/pF for MI + AAV9-NC and −35.8 ± 1.5 pA/pF for AAV9-Meis1. These data suggest that Meis1 overexpression is able to improve cardiac electrical conduction of MI hearts by recovering I_{Na} currents and producing anti-arrhythmic effects. In addition, we also constructed the knock-down of Meis1 in mouse cardiomyocytes through AAV9 to further verify the regulation of Meis1 on sodium current. As expected, the average I_{Na} densities, from test potentials of −50 mV to 0 mV, were significantly lower in AAV9-shMeis1 myocytes compared with AAV9-shNC group (−23.3 ± 2.5 pA/pF vs. −39.6 ± 1.7 pA/pF at −35 mV, $P < 0.05$, Fig. 3E,F).

Meis1 rescues the reduction of $Na_V1.5$ channel in cardiomyocytes of MI mice

The above data indicates that Meis1 could prevent ischemic arrhythmias after MI by restoring cardiac conduction velocity. It has been demonstrated that the restraint or functional impairment of $Na_V1.5$/*SCN5A* is the key inducement to slow down cardiac conduction in hearts [9,30]. Therefore, we further experimentally verify if Meis1 altered $Na_V1.5$ expression in cardiomyocytes from the marginal area of the infarcted hearts. As illustrated in Fig. 4A and B, consistent with the changes of *SCN5A* mRNA, $Na_V1.5$ protein expression was markedly down-regulated by approximately 50% in the hearts of MI group mice, which was attenuated significantly by AAV9-Meis1 administration in MI mouse hearts. This indicates that Meis1 prevents the decrease of I_{Na} current in ischemic hearts by up-regulating the $Na_V1.5$ protein level.

Furthermore, we also found that Meis1 increased the mRNA level of *SCN5A* in neonatal mouse cardiomyocytes exposed to hypoxia (Fig. 4C). Hypoxia treatment also significantly reduced the protein level of $Na_V1.5$, which was attenuated by overexpression of Meis1 in hypoxic cardiomyocytes (Fig. 4D). Similarly, the $Na_V1.5$ protein in the plasma membrane of neonatal mouse cardiomyocytes of the Hypoxia + Meis1 group was increased compared to the hypoxic cells observed by immunofluorescence technique (Fig. 4E).

The proximal promoter region of SCN5A DNA contains conserved Meis1 binding sites

The changes in mRNA and protein expression levels of the *SCN5A* gene in ischemic hearts indicates that transcription of *SCN5A* may be directly regulated by Meis1 in cardiomyocytes. Computational prediction of the high-quality and matrix-based transcription factor binding site profiles in the proximal region of the *SCN5A* promoter (2000 nt upstream) based on JASPAR database (JASPAR^{2020}, http://jaspar.genereg.net/), in which includes seven highly conserved binding sites of Meis1, and chromatin immunoprecipitation (ChIP) assays were used to verify the predicted binding sites (Fig. 5A, B). As shown in Fig. 5B, the recruitment of Meis1 to the proximal promoter region of *SCN5A* DNA in mouse ventricular tissues, which was significantly reduced in MI group mice compared with sham-operated mice. With the effectively silencing and overexpressing of Meis1 in primary cultured neonatal cardiomyocytes by si-Meis1 and Meis1 plasmid transfection (Fig. 5C, D), the expression of $Na_V1.5$ mRNA and protein was consistent with that of Meis1 (Fig. 5E, F). These results indicate that the transcription factor Meis1 has the potential to regulate transcriptional expression of *SCN5A*.

Hypoxia destabilizes Meis1 by promoting its ubiquitin proteasome dependent degradation

It was previously reported that the half-life of Meis1 was prolonged and blocked from entering ubiquitin proteasome-mediated degradation in leukemia model [31]. Nevertheless, there is little evidence indicating whether Meis1 might be dysregulated through ubiquitination pathways in cardiomyocytes. To understand the underlying mechanisms leading to the prompt degradation of Meis1 after hypoxia, we firstly examined the stability of Meis1 protein in normoxic and hypoxic cardiomyocytes. Indeed, after the protein was inhibited by cycloheximide (CHX), the half-life of Meis1 protein in the normxia group was about 12 h, whereas this declined to approximately 6 h under hypoxia treatment (Fig. 6A), suggesting that the Meis1 protein was more unstable in hypoxic cardiomyocytes than in normoxic condition. Importantly, the effect of hypoxia on Meis1 was restrained in the presence of the proteasome inhibitor MG132 in cardiomyocytes (Fig. 6B). Subsequently, the ubiquitination status of Meis1 in cardiomyocytes upon hypoxia treatment was analyzed through co-inmunoprecipitation, which confirmed that the ubiquitination level was extensively enhanced in comparison with the control group (Fig. 6C). These findings indicate that the ubiquitin proteasome pathway is involved in the hypoxia mediated down-regulation of Meis1.

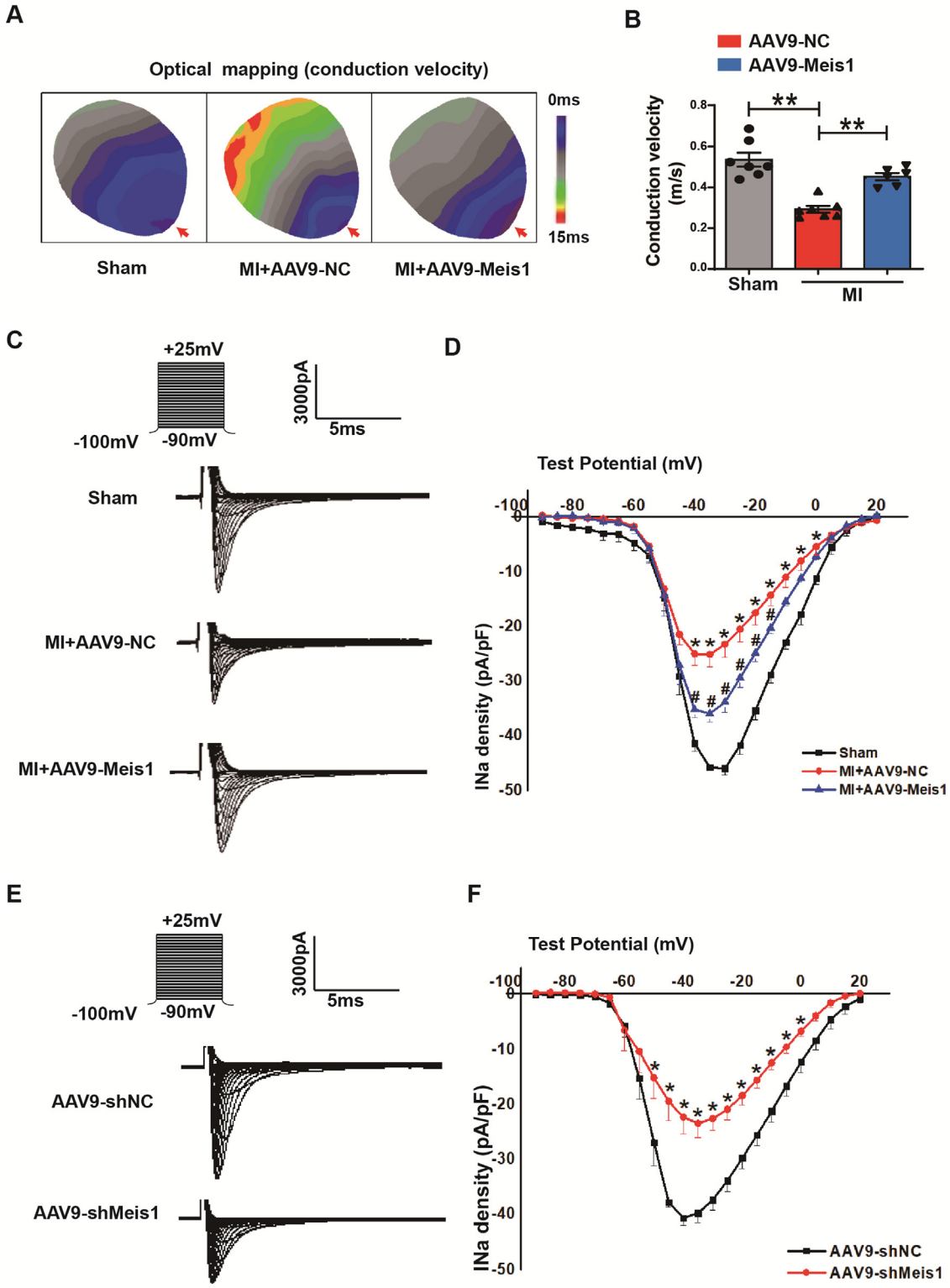

Fig. 3. Effect of Meis1 on cardiac electrical conduction in mouse hearts with MI. **(A)** Representative image of epicardial conduction recorded by optical mapping in Sham, MI + AAV9-NC and MI + AAV9-Meis1 group. The color bar indicates the activation time in milliseconds (ms). The arrows represent the electrode stimulation position. **(B)** Statistical data of conduction velocity in mouse hearts (n = 6–7). The data showed that cardiac conduction was slowed down in mice with MI, which was reversed by the overexpression of Meis1, $^{**}P < 0.01$. **(C)** Representative whole cell I_{Na} traces were recorded at the potentials between −90 mV and +25 mV from a holding potential of −100 mV in the left ventricular myocytes isolated from Sham, MI + AAV9-NC and MI + AAV9-Meis1 group. **(D)** The current-density-voltage relationship curves of I_{Na} indicated that the current densities were obviously reduced in MI + AAV9-NC group, which were restored in the AAV9-Meis1 mice hearts at the potential of −40 mV to −15 mV. $^{*}P < 0.05$ vs. Sham group; $\#P < 0.05$ vs. MI + AAV9-NC group, n = 5 mice. **(E-F)** The average sodium current densities were significantly lower in AAV9-shMeis1 myocytes compared with AAV9-shNC group at −50 mV to 0 mV, Two-tailed Student's t-test was used to compare the differences between the two experimental groups, mean ± SEM, $^{*}P < 0.05$, n = 6 mice.

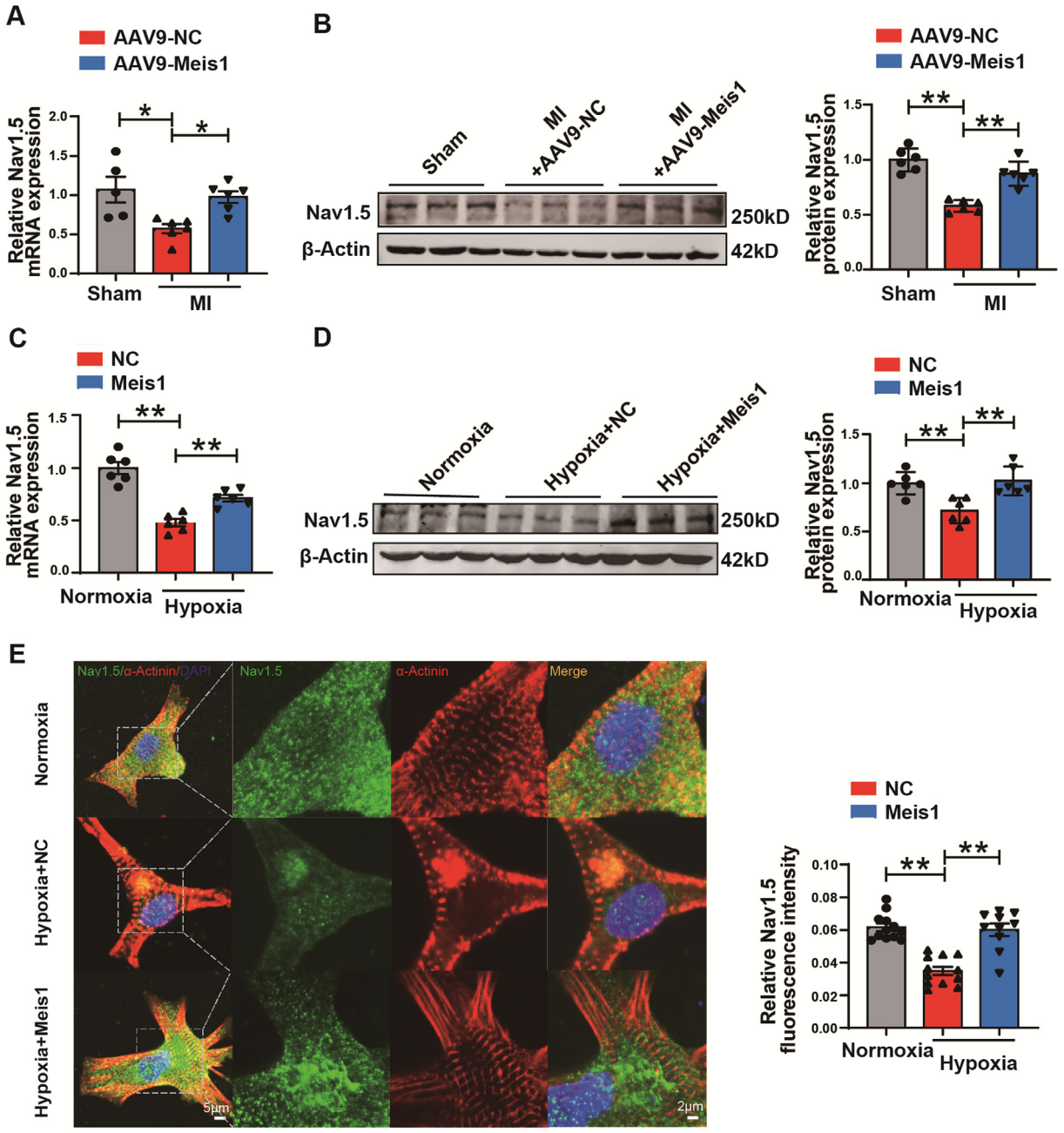

Fig. 4. Meis1 inhibits the down-regulation of *SCN5A*/$Na_V1.5$ expression in MI hearts and hypoxic cardiomyocytes. **(A-B)** The mRNA and protein expression of sodium channel subunit *SCN5A*/$Na_V1.5$ in the border zone of infracted hearts from Sham, MI + AAV9-NC and MI + AAV9-Meis1 group (n = 6). **(C-D)** The expression of *SCN5A*/$Na_V1.5$ at mRNA and protein level in neonatal mouse cardiomyocytes after treatment with hypoxia for 24 h with or without forced expression of Meis1 (n = 6). **(E)** Immunofluorescence staining for $Na_V1.5$ (green), α-actinin (red) proteins in neonatal mouse cardiomyocytes after treatment with hypoxia for 24 h with or without overexpression of Meis1 (left panels) and enlargement of outlined squares (right panels). Scale bar indicates 5 μm/2 μm. One-way ANOVA was used to determine statistical significance in these experiments. Error bars represent mean ± SEM of each group. $^*P < 0.05$, $^{**}P < 0.01$. (For interpretation of the references to color in this figure legend, the reader is referred to the web version of this article.)

CDC20 promotes Meis1 ubiquitination and degradation in cardiomyocytes

The ubiquitin-proteasome system is essential for protein homeostasis. The interaction between E3 ubiquitin ligase and the target protein is a core step of protein degradation mediated by the ubiquitin-proteasome system [32]. E3 ubiquitin ligase mediates the destruction of homologous substrates by adding ubiquitin to the lysine residues of the substrates. Therefore, we firstly used UbiBrowser database (http://ubibrowser.ncpsb.org/) and real-time PCR assay to identify the potential E3 ubiquitin ligases interacting with Meis1. As shown in Fig. 7A, compared with other ligases, CDC20 mRNA expression was found markedly up-regulated in MI mouse hearts. Moreover, CDC20 protein levels were also increased in both MI mouse hearts and neonatal mouse cardiomyocytes after exposure to hypoxia (Fig. 7B, C). Since the expression of CDC20 is up-regulated in ischemic and hypoxic cardiomyocytes, we speculated that CDC20 may be the key E3 enzyme of Meis1 to regulate its ubiquitin-proteasome degradation. Firstly, we evaluated whether CDC20 is responsible for Meis1 protein degradation in ischemic cardiomyocytes. Compared with the si-NC group, knockdown of CDC20 in cardiomyocytes via siRNA appreciably enhanced Meis1 and $Na_V1.5$ protein levels after 24 h of hypoxia treatment (Fig. 7D). Conversely, overexpression of CDC20 reduced the level

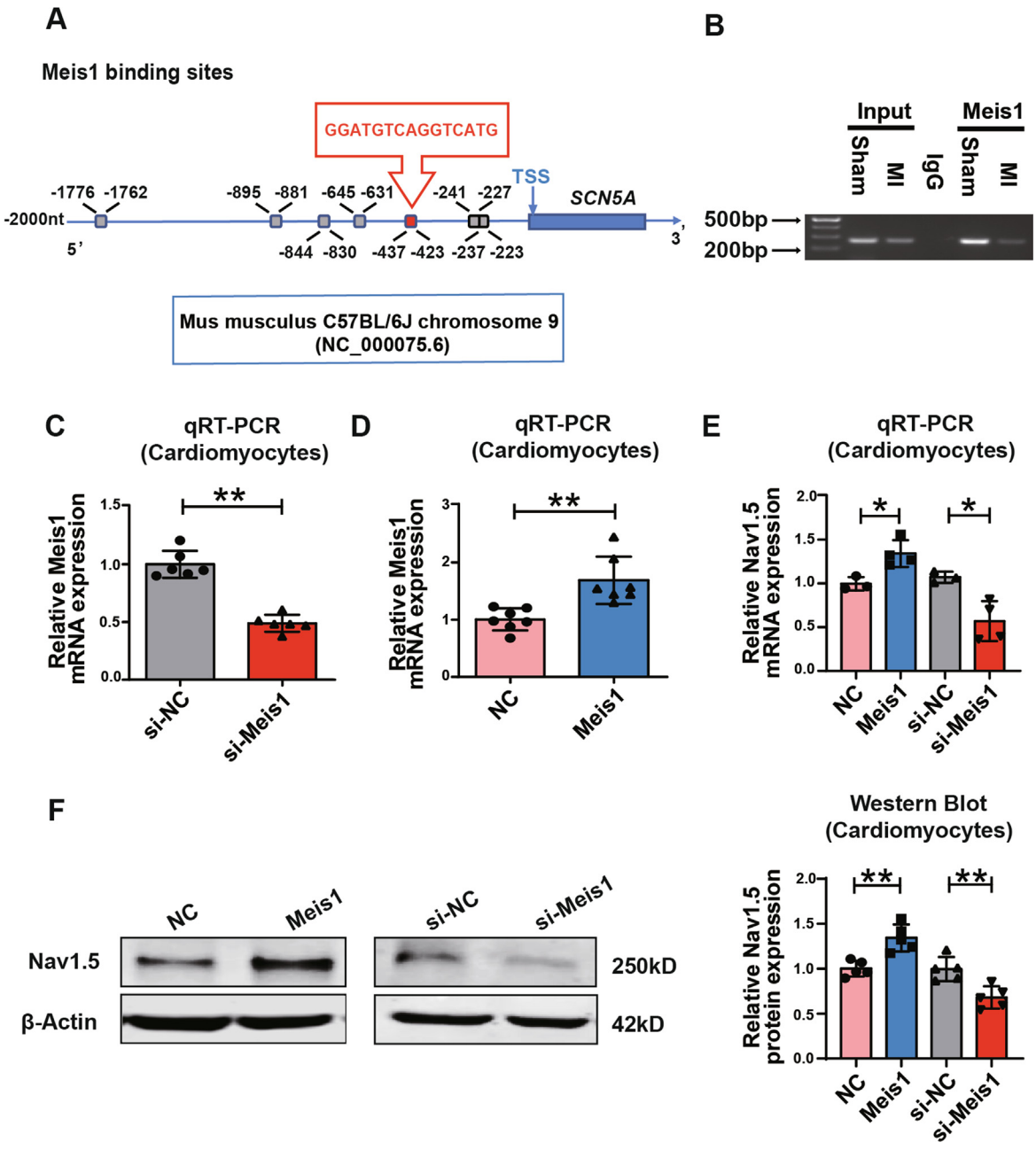

Fig. 5. The *SCN5A* DNA promoter region contains conserved Meis1 binding sites. **(A)** Conservative Meis1 binding sites in the proximal region (2000 nt upstream) of *SCN5A* DNA promoter computational predicted by JASPAR database (JASPAR[2020]). **(B)** ChIP assay was performed by using antibody against Meis1, and IgG as control on the mice ventricular myocardium in sham or MI group. **(C-D)** Real-time PCR was performed to evaluate the expression of Meis1 mRNA in neonatal mouse cardiomyocytes by knockdown of Meis1 with si-Meis1 or overexpressed of Meis1 by plasmid. At least six independent batches of cells for each group, $^{**}P < 0.01$. **(E-F)** The mRNA and protein levels of sodium channel subunit *SCN5A*/$Na_V1.5$ in neonatal mouse cardiomyocytes of NC, si-NC, si-Meis1 and Meis1 group (n = 3–5). Two-tailed student's *t*-test was performed. $^{*}P < 0.05$, $^{**}P < 0.01$.

of Meis1 and $Na_V1.5$ protein compared with the hypoxia alone treatment group (Fig. 7E). These results suggest that CDC20 is involved in regulation of Meis1 stability in hypoxic cardiomyocytes.

CDC20 involves the protective effect of Meis1 on ischemic-induced $Na_V1.5$ reduction

Moreover, after co-transfected with Flag-Meis1 and His-CDC20 plasmids in HEK293T cells for 48 h, we found that Meis1 could be detected upon CDC20 pull down by co-immunoprecipitation assay (Fig. 8A). The result of pull-down assay indicated that a physical interaction between Meis1 and CDC20 in cardiomyocytes. Moreover, the endogenous CDC20 protein could be effectively precipitated by anti-Meis1 antibody (Fig. 8B). To determine whether CDC20 reduced the stability of Meis1 through the ubiquitin proteasome pathway, IP technique was performed with Meis1 antibody in neonatal mouse cardiomyocytes. The results showed that overexpression of CDC20 significantly enhanced the ubiquitination level and degradation of Meis1 (Fig. 8C). On the contrary, silencing of CDC20 reduced Meis1 ubiquitination and degradation compared with the si-NC group (Fig. 8D). These results indicate that CDC20 regulates ubiquitination of Meis1 directly. Furthermore, we also

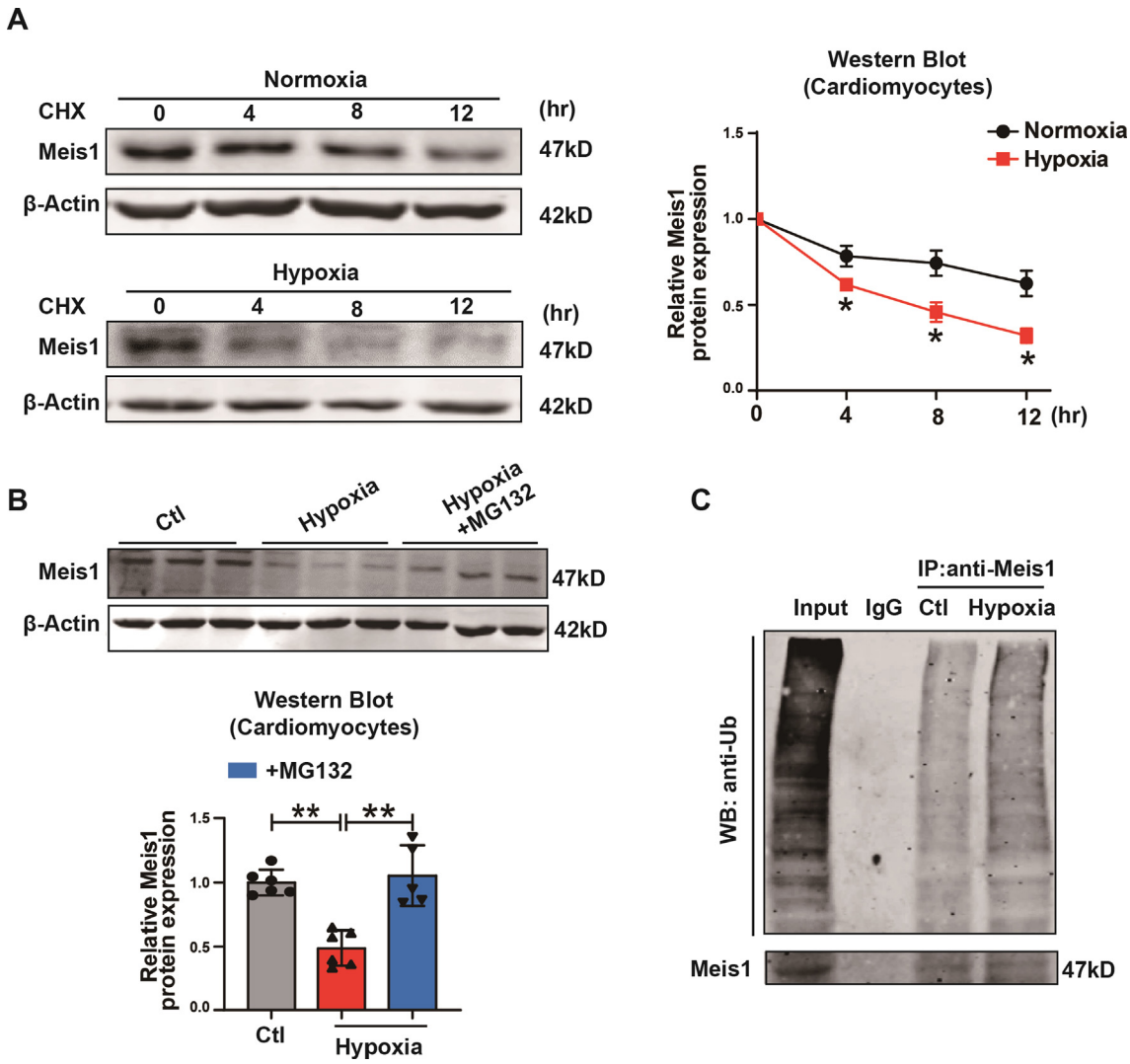

Fig. 6. Meis1 is degraded by the ubiquitin proteasome pathway. **(A)** The Meis1 level was evaluated by immunoblotting in a chase experiment using cycloheximide (CHX, 0.1 mM) in cardiomyocytes upon hypoxia treatment (n = 4). **(B)** Neonatal mouse cardiomyocytes were treated with hypoxia in the presence or absence of MG132 (5 μM) for 24 h, and the protein level of Meis1 were then detected (n = 6). Error bars represent mean ± SEM of experiments. $^{*}P < 0.05$, $^{**}P < 0.01$. **(C)** Lysates collected from neonatal mousecardiomyocytes treated with hypoxia or not were immunoprecipitated with anti-Meis1 (n = 3). Ubiquitin conjugated Meis1 was detected by Western Blot assay against ubiquitin (Ub). Input representing the protein expression in whole cell lysates.

founded that the effect of CDC20 on the degradation of Meis1 was abolished in the presence of the proteasome inhibitor MG132 in cardiomyocytes (Fig. 8E). Knockdown of CDC20 by si-CDC20 increased the protein level of Meis1 compared with the si-NC treatment cells, and which is more evident after treatment with MG132 in neonatal cardiomyocytes (Fig. 8F). Overall, these results suggest that CDC20 regulates Meis1 protein levels in a ubiquitin-proteasome-dependent manner.

Next, we further explored whether CDC20 affected the expression of $Na_V1.5$ by regulating Meis1. Immunoblotting assays confirmed that the $Na_V1.5$ protein expression was increased when CDC20 was knocked down in neonatal cardiomyocytes after hypoxia treatment, which was markedly reversed by siRNA-Meis1 (Fig. 8G). It suggests that CDC20 mediates the protective effect of Meis1 on ischemic-induced $Na_V1.5$ reduction.

Discussion

Fatal arrhythmias and subsequent sudden cardiac death are the most frequent causes of death in patients with MI [33–34]. The imbalance of cardiac ion channels expression and function results in myocardial electrical remodeling after MI. For the first time, we uncovered that the up-regulation of CDC20 in ischemic cardiomyocytes after MI leads to the accelerated degradation of Meis1 in the manner of ubiquitin–proteasome system, which leads to the dysfunction of cardiac Na^+ channel (*SCN5A*/$Na_V1.5$) and then ultimately induces an increased susceptibility to arrhythmias. The finding provides novel insights into the mechanisms of ventricular arrhythmias after MI, and confers Meis1 as a new therapeutic target for sudden cardiac death.

Meis1, as a three-amino-acid loop extension (TALE) family homeobox gene, plays an important role in leukemia, tumor and cardiac regeneration [35]. It has been reported that Meis1 inactivation in mouse neurons induces the dysfunction of sympathetic and vagal regulation of cardiac rhythmicity and cardiac conduction defects, thus increasing the susceptibility to SCD [17]. Although inactivation of Meis1 has been shown to cause neurological disorders, the functions of Meis1 in the development of ventricular arrhythmias after myocardial infarction has not been reported. Here, we found that the forced expression of Meis1 could inhibit the incidence of arrhythmias and restore cardiac conduction velocity in MI mice. It suggests that Meis1 might be a new target for the treatment of arrhythmias after MI.

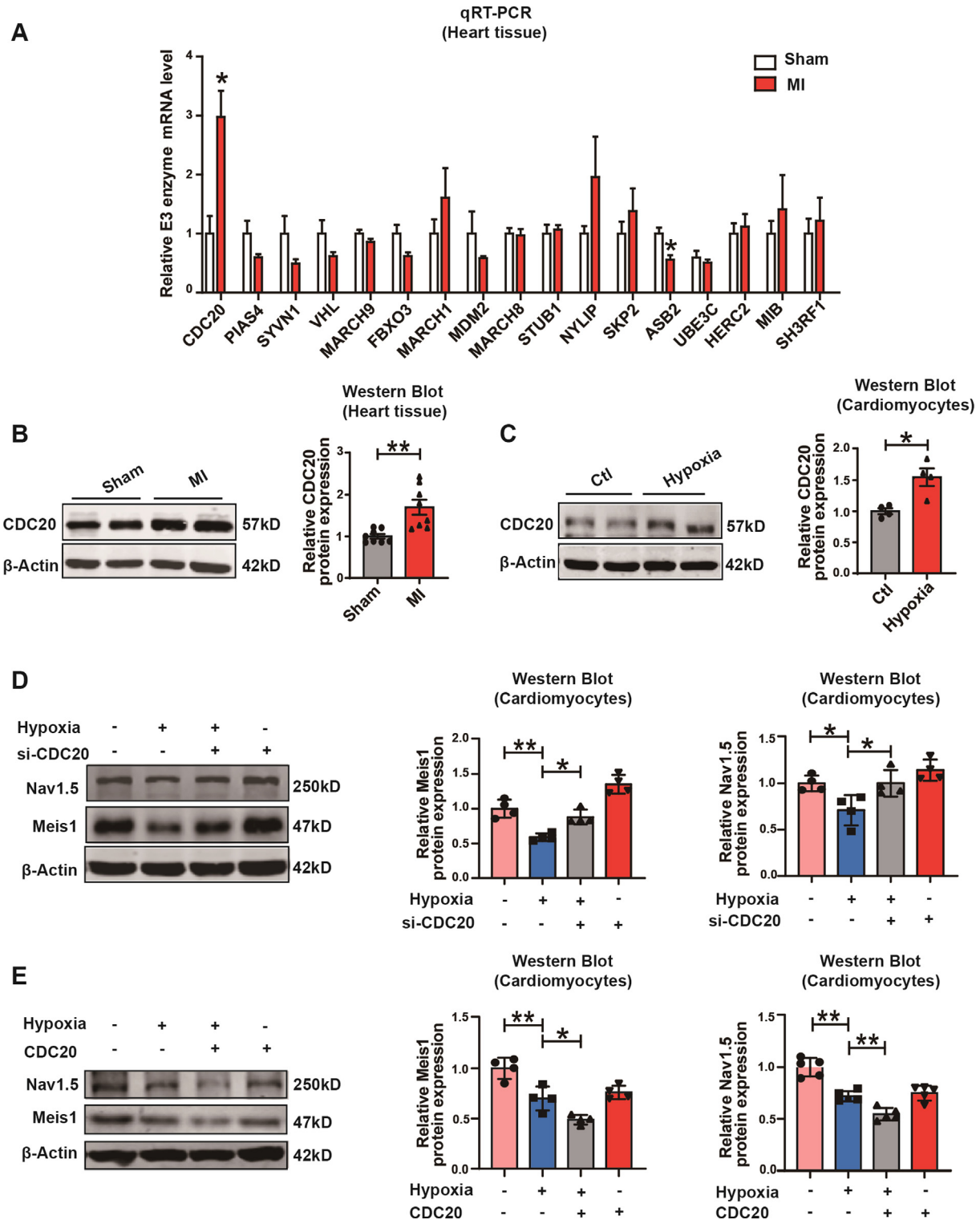

Fig. 7. CDC20 affects the stability of Meis1 in cardiomyocytes. **(A)** The expression of E3 enzyme related to Meis1 in MI and Sham group mouse hearts (n = 5) analyzed by qRT-PCR assay. $^{*}P < 0.05$ vs. Sham group. **(B)** The protein expression of CDC20 in the hearts after 4 weeks of MI (n = 8). Two-tailed student's *t*-test was performed. **(C)** The expression of CDC20 protein was increased in neonatal mouse cardiomyocytes treated with hypoxia for 24 h (n = 4). **(D)** The variation of $Na_V1.5$ and Meis1 expression in hypoxic cardiomyocytes with or without knocking down CDC20 by si-CDC20 transfection (n = 4). **(E)** The variation of $Na_V1.5$ and Meis1 expression in hypoxic cardiomyocytes after forced expression of CDC20 by CDC20-plasmid transfection (n = 4–5). One-way ANOVA was used to determine statistical significance in these experiments. Error bars represent mean ± SEM of each group. $^{*}P < 0.05$, $^{**}P < 0.01$.

It has been widely accepted that abnormal Na^+ channel affects electrical conduction and cardiac excitability, which is associated with cardiac arrhythmias after myocardial infarction, such as serious ventricular arrhythmias and LQT syndrome [36–37]. The incidence of ventricular arrhythmia in patients with loss of function of sodium channel is much higher than that in healthy individuals [38]. Consistent with previous studies, we found that the prolongation of QRS complex in MI mice was accompanied by a decrease in

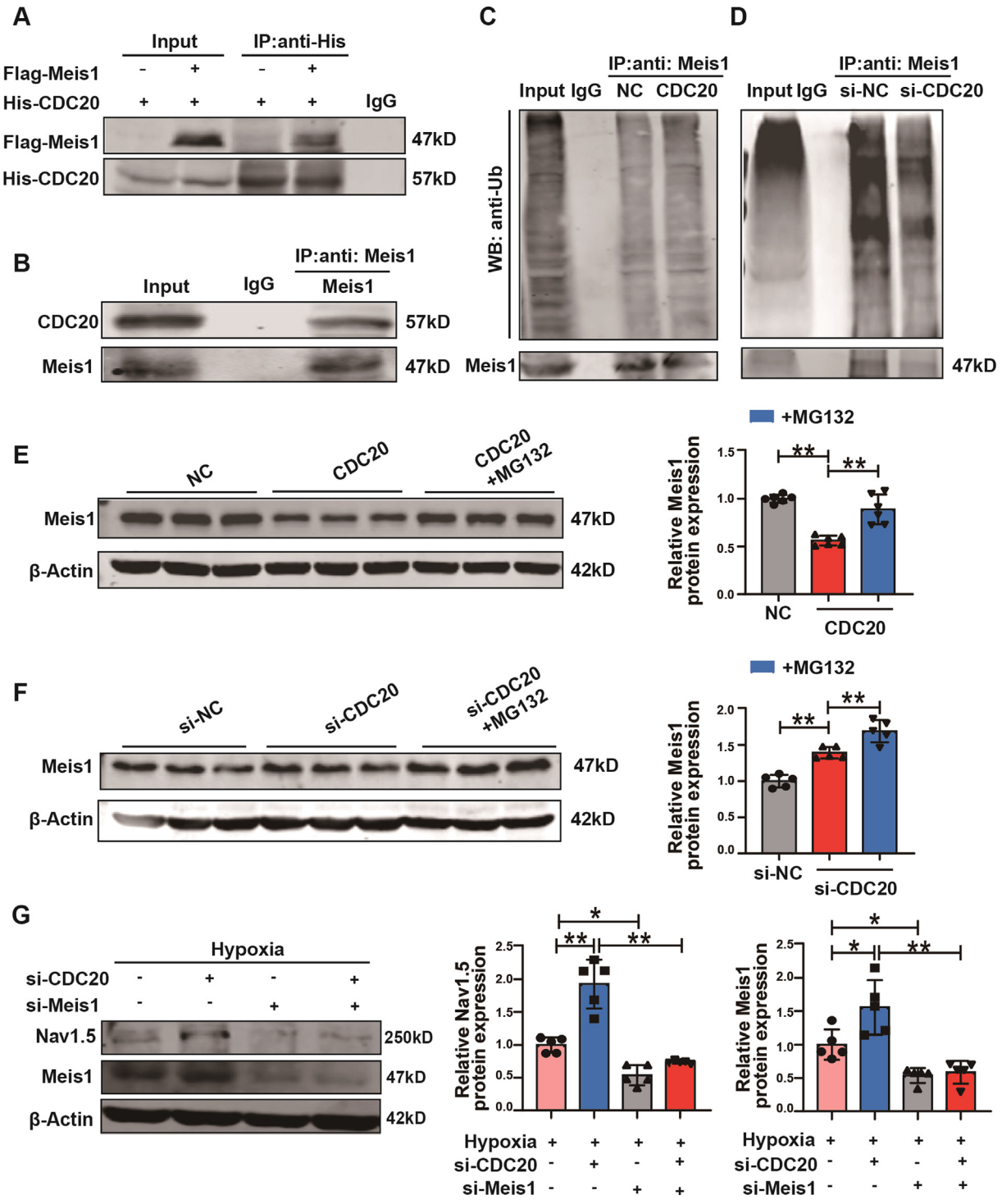

Fig. 8. CDC20 promotes Meis1 ubiquitination and degradation in cardiomyocytes. **(A)** Flag-tagged Meis1 and His-tagged CDC20 plasmid were overexpressed in HEK293T cells for 48 h, followed by immunoprecipitation with His antibody and western blotting for Flag (n = 3). **(B)** Immunoprecipitation was performed on the protein extracted from mouse ventricular myocardium by using the antibody against Meis1 and western blotting for CDC20 (n = 3). **(C-D)** Lysates collected from cardiomyocytes treated with CDC20 plasmid or si-CDC20 and pretreatment with MG132 for 24 h were immunoprecipitated with anti-Meis1. The ubiquitin-conjugated Meis1 was detected by western blotting with anti-ubiquitin (Ub). Input representing the protein expression in whole cell lysates. **(E-F)** Neonatal mouse cardiomyocytes were treated with CDC20 plasmid or si-CDC20 in the presence or absence of MG132 (5 μM) for 24 h. Representative immunoblotting analyses of Meis1 expression levels for each group (n = 5–6). **(G)** The expression of $Na_V1.5$ and Meis1 in hypoxia neonatal mouse cardiomyocytes after knocking down of CDC20 and Meis1 by si-CDC20/si-Meis1 transfection for 24 h (n = 5). One-way ANOVA was used to determine statistical significance in these experiments. Error bars represent mean ± SEM of each group. $^*P < 0.05$, $^{**}P < 0.01$.

the expression of $Na_V1.5$, α subunit of the cardiac Na^+ channel in the marginal zone of myocardial infarction in mice. However, the mechanism underlying cardiac sodium channel dysfunction in MI, especially at the transcriptional aspect, is not yet clear. Interestingly, our study showed that there are multiple binding sites between Meis1 and the promoter region of *SCN5A* DNA, and the overexpression of Meis1 could restore the reduction of $Na_V1.5$ in cardiomyocytes and reverse the QRS prolongation. Surprisingly,

we found that Meis1 could also restore the QTc (heart rate corrected QT) interval of the infarcted heart, indicating that Meis1 might also participate in the repolarization process of the heart. Potassium current (I_k) and calcium current (I_{Ca}) cooperate with I_{Na} to mediate the process of orderly electrical activity of the heart. Here we firstly revealed the transcriptional regulation mechanism of sodium channel (*SCN5A*/$Na_V1.5$) mediated by Meis1 during myocardial infarction. However, we cannot exclude a potential contribution of Meis1 function on other ion channels which should be defined in future studies. In addition, the electrical conduction of the heart is affected by both intracellular conduction and intercellular communication. Connexin43 (Cx43), has been identified as essential for the cell-to-cell transmission of action potential in cardiomyocytes, which co-determines cardiac depolarization with sodium channel activation [39]. Here, we also observed the effects of Meis1 on Connexin43 in the hearts of each group mice. However, the results displayed that the overexpression of Meis1 could not restore the downregulation of Connexin43 protein in infarcted hearts (**Supplementary** Fig. 2A). This suggested that the effect of Meis1 on cardiac conduction might be more specific to sodium currents rather than the cardiac gap junction.

Meis1 has been showed to be involved in the vascularization of ischemic myocardial tissue and inhibit angiotensin II-induced myocardial hypertrophy by promoting the expression of Poly (rC)-binding protein 2 [40]. Fabrice et al. also reported that the loss of transcription factor Meis1 increases the sensitivity to sudden cardiac death by inhibiting the sympathetic neurons target-field innervation [17]. In this study, we demonstrated that the downregulation of Meis1 in cardiomyocytes reduced the transcriptional regulation of *SCN5A*, which eventually lead to the increased susceptibility of arrhythmias in mice after MI.

However, the mechanism leading to the down regulation of Meis1 in this pathological process still undefined. In the current study, we discovered that the degradation of Meis1 protein was accelerated in MI mouse hearts and hypoxic cardiomyocytes by the ubiquitin proteasome pathway. Previous studies have found that E3 ubiquitin ligase CDC20 significantly increased K48-linked ubiquitination level and Meis1 degradation in leukemia models [26]. Increasing evidence indicates that CDC20 binds directly to LC3 and promotes the ubiquitination and degradation of LC3 through proteasome, thus inhibiting cardiac autophagy and hypertrophy [41]. However, whether CDC20 regulates the proteasomal degradation of Meis1 in ischemic cardiomyocytes is unknown. Here, were found that the expression of CDC20 was up-regulated in the border zone of infracted hearts and hypoxic cardiomyocytes. After hypoxia stimulation, knockdown of CDC20 in cardiomyocytes restored the expression of $Na_V1.5$ and Meis1, but overexpression of CDC20 exacerbated their down-regulation, demonstrating that CDC20 exerts an important regulatory effect on sodium channel ($Na_V1.5$) and Meis1 in cardiomyocytes.

We then further investigated whether Meis1 degraded through the ubiquitination regulation of CDC20. In this study, we revealed for the first time the binding relationship between Meis1 and CDC20 in cardiomyocytes of MI mice. At the same time, it was found that Meis1 did degrade through the ubiquitination of CDC20 under the stimulation of hypoxia, and thus failed to exert the regulation of $Na_V1.5$. Our findings furnish original mechanistic insights into the probably links amongst CDC20 and Meis1 regulating $Na_V1.5$ in cardiomyocytes.

Conclusions

In summary, the present study is the first to investigate the regulatory effect of Meis1 on arrhythmia in adult mice with myocardial infarction. The expression of Meis1 was down-regulated in ischemic cardiomyocytes, which may be mainly caused by CDC20-mediated ubiquitination. After the Meis1 level was restored, the electrophysiological function in marginal zone of infarcted mouse hearts and I_{Na} current density in cardiomyocytes were significantly improved. It provides strong evidences that Meis1 has the anti-arrhythmic effects by mediating *SCN5A* in the process of myocardial infarction. These findings confer novel therapeutic strategies for MI complicated with malignant arrhythmias and sudden cardiac death.

Compliance with Ethics Requirements

This research has fully complied with research ethics. All animal experiments were performed along with the NIH guidelines (Guide for the care and use of laboratory animals, NIH Publication No. 85-23, revised 1996) and the ARRIVE guidelines. All experiments were conducted in accordance with the protocols approved by the Institutional Animal Care and Use Committee of Harbin Medical University.

CRediT authorship contribution statement

Yining Liu: Writing – original draft, Investigation, Validation, Visualization, Methodology, Formal analysis. **Jiamin Li:** Methodology, Conceptualization. **Ning Xu:** Methodology, Investigation, Validation. **Hang Yu:** Validation, Investigation. **Liling Gong:** Investigation, Formal analysis. **Qingsui Li:** Investigation, Data curation. **Zhenyu Yang:** Methodology, Investigation, Validation. **Sijia Li:** Investigation, Formal analysis. **Jiming Yang:** Investigation, Validation. **Di Huang:** Formal analysis. **Yadong Xue:** Investigation, Validation. **Genlong Xue:** Investigation, Validation. **Jiali Liu:** Investigation. **Haixin Chen:** Methodology, Investigation. **Ruijie Zhang:** Formal analysis. **Anqi Li:** Methodology, Investigation. **Yiming Zhao:** Investigation. **PengYu Li:** Data curation. **Ming Li:** Methodology. **Mingbin Liu:** Validation, Formal analysis. **Benzhi Cai:** Conceptualization, Writing – original draft. **Ning Wang:** Visualization, Writing – original draft, Conceptualization, Supervision, Project administration.

Declaration of Competing Interest

The authors declare that they have no known competing financial interests or personal relationships that could have appeared to influence the work reported in this paper.

Acknowledgements

This work was supported by Heilongjiang Touyan Innovation Team Program [NW, BZC]; HMU Marshal Initiative Funding [Grant No. HMUMIF-21026 to NW]; the National Nature Science Foundation of China [Grant No. 82170284 and 81773733 to NW]; National Nature Science Youth Foundation of China [Grant No. 82003751 to JML]; Foundation of Heilongjiang postdoctoral [LBH-Z18166 to JML] and Outstanding Youth Fostering Foundation of Vihan Academician [NW]. The mechanism diagram was created with BioRender.com.

Appendix A. Supplementary material

Supplementary data to this article can be found online at https://doi.org/10.1016/j.jare.2021.11.004.

References

[1] Bigger JT, Fleiss JL, Kleiger R, Miller JP, Rolnitzky LM. The relationships among ventricular arrhythmias, left ventricular dysfunction, and mortality in the 2 years after myocardial infarction. Circulation 1984;69(2):250–8.

[2] Aimond F, Alvarez JL, Rauzier JM, Lorente P, Vassort G. Ionic basis of ventricular arrhythmias in remodeled rat heart during long-term myocardial infarction. Cardiovasc Res 1999;42(2):402–15.
[3] Daya MR, Leroux BG, Dorian P, Rea TD, Newgard CD, Morrison LJ, et al. Survival After Intravenous Versus Intraosseous Amiodarone, Lidocaine, or Placebo in Out-of-Hospital Shock-Refractory Cardiac Arrest. Circulation 2020;141(3):188–98.
[4] Shy D, Gillet L, Abriel H. Cardiac sodium channel NaV1.5 distribution in myocytes via interacting proteins: the multiple pool model. Biochim Biophys Acta 2013;1833(4):886–94.
[5] Liu M, Yang KC, Dudley Jr SC. Cardiac Sodium Channel Mutations: Why so Many Phenotypes? Curr Top Membr 2016;78:513–59.
[6] Wagner S, Maier LS, Bers DM. Role of sodium and calcium dysregulation in tachyarrhythmias in sudden cardiac death. Circ Res 2015;116(12):1956–70.
[7] Pu J, Boyden PA. Alterations of Na+ currents in myocytes from epicardial border zone of the infarcted heart. A possible ionic mechanism for reduced excitability and postrepolarization refractoriness. Circ Res 1997;81(1):110–9.
[8] Baba S, Dun W, Cabo C, Boyden PA. Remodeling in cells from different regions of the reentrant circuit during ventricular tachycardia. Circulation 2005;112(16):2386–96.
[9] Li J, Xu C, Liu Y, Li Y, Du S, Zhang R, et al. Fibroblast growth factor 21 inhibited ischemic arrhythmias via targeting miR-143/EGR1 axis. Basic Res Cardiol 2020;115(2). doi: https://doi.org/10.1007/s00395-019-0768-4.
[10] Shang LL, Pfahnl AE, Sanyal S, Jiao Z, Allen J, Banach K, et al. Human heart failure is associated with abnormal C-terminal splicing variants in the cardiac sodium channel. Circ Res 2007;101(11):1146–54.
[11] Veerman CC, Wilde AAM, Lodder EM. The cardiac sodium channel gene SCN5A and its gene product NaV1.5: Role in physiology and pathophysiology. Gene 2015;573(2):177–87.
[12] Roychoudhury J, Clark JP, Gracia-Maldonado G, Unnisa Z, Wunderlich M, Link KA, et al. MEIS1 regulates an HLF-oxidative stress axis in MLL-fusion gene leukemia. Blood 2015;125(16):2544-52.
[13] Su Z, Si W, Li L, Zhou B, Li X, Xu Y, et al. MiR-144 regulates hematopoiesis and vascular development by targeting meis1 during zebrafish development. Int J Biochem Cell Biol 2014;49:53–63.
[14] Mahmoud AI, Kocabas F, Muralidhar SA, Kimura W, Koura AS, Thet S, et al. Meis1 regulates postnatal cardiomyocyte cell cycle arrest. Nature 2013;497(7448):249–53.
[15] Islam MM, Li Y, Luo H, Xiang M, Cai L. Meis1 regulates Foxn4 expression during retinal progenitor cell differentiation. Biol Open 2013;2(11):1125–36.
[16] Nguyen NUN, Canseco DC, Xiao F, Nakada Y, Li S, Lam NT, et al. A calcineurin-Hoxb13 axis regulates growth mode of mammalian cardiomyocytes. Nature 2020;582(7811):271–6.
[17] Bouilloux F, Thireau J, Venteo S, Farah C, Karam S, Dauvilliers Y, et al. Loss of the transcription factor Meis1 prevents sympathetic neurons target-field innervation and increases susceptibility to sudden cardiac death. Elife 2016;5.
[18] Pfeufer A, van Noord C, Marciante KD, Arking DE, Larson MG, Smith AV, et al. Genome-wide association study of PR interval. Nat Genet 2010;42(2):153–9.
[19] Smith JG, Magnani JW, Palmer C, Meng YA, Soliman EZ, Musani SK, et al. Genome-wide association studies of the PR interval in African Americans. PLoS Genet 2011;7(2):e1001304.
[20] Reithmann C, Hoffmann E, Grunewald A, Nimmermann P, Remp T, Dorwarth U, et al. Fast pathway ablation in patients with common atrioventricular nodal reentrant tachycardia and prolonged PR interval during sinus rhythm. Eur Heart J 1998;19(6):929–35.
[21] Wang X, Robbins J. Heart failure and protein quality control. Circ Res 2006;99(12):1315–28.
[22] Mearini G, Schlossarek S, Willis MS, Carrier L. The ubiquitin-proteasome system in cardiac dysfunction. Biochim Biophys Acta 2008;1782(12):749–63.
[23] Barac YD, Emrich F, Krutzwakd-Josefson E, Schrepfer S, Sampaio LC, Willerson JT, et al. The ubiquitin-proteasome system: A potential therapeutic target for heart failure. J Heart Lung Transplant 2017;36(7):708–14.
[24] Nakayama KI, Nakayama K. Ubiquitin ligases: cell-cycle control and cancer. Nat Rev Cancer 2006;6(5):369–81.
[25] Amador V, Ge S, Santamaría PG, Guardavaccaro D, Pagano M. APC/C(Cdc20) controls the ubiquitin-mediated degradation of p21 in prometaphase. Mol Cell 2007;27(3):462–73.
[26] Liu X, Zhang F, Zhang Y, Li X, Chen C, Zhou M, et al. PPM1K Regulates Hematopoiesis and Leukemogenesis through CDC20-Mediated Ubiquitination of MEIS1 and p21. Cell Rep 2018;23(5):1461–75.
[27] Yu Z, Zhang Hu, Yu M, Ye Q. Analysis of Gene Expression During the Development of Congestive Heart Failure After Myocardial Infarction in Rat Models. Int Heart J 2015;56(4):444–9.
[28] Lindsey ML, Bolli R, Canty JM, Du X-J, Frangogiannis NG, Frantz S, et al. Guidelines for experimental models of myocardial ischemia and infarction. Am J Physiol Heart Circ Physiol 2018;314(4):H812–38.
[29] Wang N, Huo R, Cai B, Lu Y, Ye B, Li X, et al. Activation of Wnt/beta-catenin signaling by hydrogen peroxide transcriptionally inhibits NaV1.5 expression. Free Radic Biol Med 2016;96:34–44.
[30] Kelly A, Salerno S, Connolly A, Bishop M, Charpentier F, Stolen T, et al. Normal interventricular differences in tissue architecture underlie right ventricular susceptibility to conduction abnormalities in a mouse model of Brugada syndrome. Cardiovasc Res 2018;114(5):724-36.
[31] Garcia-Cuellar M-P, Steger J, Fuller E, Hetzner K, Slany RK. Pbx3 and Meis1 cooperate through multiple mechanisms to support Hox-induced murine leukemia. Haematologica 2015;100(7):905–13.
[32] Morreale FE, Walden H. Types of Ubiquitin Ligases. Cell 2016;165(1):248–248.e1.
[33] Solomon SD, Zelenkofske S, McMurray JJV, Finn PV, Velazquez E, Ertl G, et al. Sudden death in patients with myocardial infarction and left ventricular dysfunction, heart failure, or both. N Engl J Med 2005;352(25):2581–8.
[34] Gholamzadeh A, Amini S, Mohammadpour AH, Vahabzadeh M, Fazelifar AF, Fazlinezhad A, et al. Erythropoietin Reduces Post-PCI Arrhythmias in Patients With ST-elevation Myocardial Infarction. J Cardiovasc Pharmacol 2015;65(6):555–61.
[35] Aksoz M, Turan RD, Albayrak E, Kocabas F. Emerging Roles of Meis1 in Cardiac Regeneration, Stem Cells and Cancer. Curr Drug Targets 2018;19(2):181–90.
[36] Remme CA, Bezzina CR. Sodium channel (dys)function and cardiac arrhythmias. Cardiovasc Ther 2010;28(5):287–94.
[37] Waddell-Smith KE, Skinner JR, Bos JM. Pre-Test Probability and Genes and Variants of Uncertain Significance in Familial Long QT Syndrome. Heart Lung Circ 2020;29(4):512–9.
[38] Hu D, Viskin S, Oliva A, Carrier T, Cordeiro JM, Barajas-Martinez H, et al. Novel mutation in the SCN5A gene associated with arrhythmic storm development during acute myocardial infarction. Heart Rhythm 2007;4(8):1072–80.
[39] Lawrence TS, Beers WH, Gilula NB. Transmission of hormonal stimulation by cell-to-cell communication. Nature 1978;272(5653):501–6.
[40] Zhang Y, Si Yi, Ma N. Meis1 promotes poly (rC)-binding protein 2 expression and inhibits angiotensin II-induced cardiomyocyte hypertrophy. IUBMB Life 2016;68(1):13–22.
[41] Xie Y-P, Lai S, Lin Q-Y, Xie X, Liao J-W, Wang H-X, et al. CDC20 regulates cardiac hypertrophy via targeting LC3-dependent autophagy. Theranostics 2018;8(21):5995–6007.